

University of Wollongong

Research Online

Australian Institute for Innovative Materials -
Papers

Australian Institute for Innovative Materials

1-1-2013

Atomic and electronic structures of single-layer FeSe on SrTiO₃(001): The role of oxygen deficiency

Junhyeok Bang

Rensselaer Polytechnic Institute

Zhi Li

Chinese Academy of Sciences, zhili@uow.edu.au

Y Y. Sun

Rensselaer Polytechnic Institute

Amit Samanta

Princeton University

Y Y. Zhang

Rensselaer Polytechnic Institute

See next page for additional authors

Follow this and additional works at: <https://ro.uow.edu.au/aiimpapers>



Part of the [Engineering Commons](#), and the [Physical Sciences and Mathematics Commons](#)

Recommended Citation

Bang, Junhyeok; Li, Zhi; Sun, Y Y.; Samanta, Amit; Zhang, Y Y.; Zhang, Wenhao; Wang, Lili; Chen, Xi; Ma, Xu-Cun; Xue, Qi-Kun; and Zhang, S B., "Atomic and electronic structures of single-layer FeSe on SrTiO₃(001): The role of oxygen deficiency" (2013). *Australian Institute for Innovative Materials - Papers*. 2627. <https://ro.uow.edu.au/aiimpapers/2627>

Research Online is the open access institutional repository for the University of Wollongong. For further information contact the UOW Library: research-pubs@uow.edu.au

Atomic and electronic structures of single-layer FeSe on SrTiO₃(001): The role of oxygen deficiency

Abstract

Using first-principles calculation, we propose an interface structure for single triple-layer FeSe on the SrTiO₃(001) surface, a high-T_c superconductor found recently. The key component of this structure is the oxygen deficiency on the top layer of the SrTiO₃ substrate, as a result of Se etching used in preparing the high-T_c samples. The O vacancies strongly bind the FeSe triple layer to the substrate giving rise to a (2 × 1) reconstruction, as observed by scanning tunneling microscopy. The enhanced binding correlates to the significant increase of T_c observed in experiment. The O vacancies also serve as the source of electron doping, which modifies the Fermi surface of the first FeSe layer by filling the hole pocket near the center of the surface Brillouin zone, as suggested from angle-resolved photoemission spectroscopy measurement.

Keywords

role, sratio3(001);, fese, single-layer, structures, deficiency, electronic, oxygen, atomic

Disciplines

Engineering | Physical Sciences and Mathematics

Publication Details

Bang, J., Li, Z., Sun, Y. Y., Samanta, A., Zhang, Y. Y., Zhang, W., Wang, L., Chen, X., Ma, X., Xue, Q. & Zhang, S. B. (2013). Atomic and electronic structures of single-layer FeSe on SrTiO₃(001): The role of oxygen deficiency. *Physical Review B: Condensed Matter and Materials Physics*, 87 220503-1-220503-4.

Authors

Junhyeok Bang, Zhi Li, Y Y. Sun, Amit Samanta, Y Y. Zhang, Wenhao Zhang, Lili Wang, Xi Chen, Xu-Cun Ma, Qi-Kun Xue, and S B. Zhang



Atomic and electronic structures of single-layer FeSe on SrTiO₃(001): The role of oxygen deficiency

Junhyeok Bang,¹ Zhi Li,² Y. Y. Sun,^{1,*} Amit Samanta,³ Y. Y. Zhang,¹ Wenhao Zhang,⁴ Lili Wang,² X. Chen,⁴ Xucun Ma,² Q.-K. Xue,^{2,4,†} and S. B. Zhang^{1,‡}

¹*Department of Physics, Applied Physics and Astronomy, Rensselaer Polytechnic Institute, Troy, New York 12180, USA*

²*Institute of Physics, The Chinese Academy of Sciences, Beijing 100190, China*

³*Program in Applied and Computational Mathematics, Princeton University, Princeton, New Jersey 08544, USA*

⁴*Department of Physics, Tsinghua University, Beijing 100084, China*

(Received 4 January 2013; revised manuscript received 28 May 2013; published 6 June 2013)

Using first-principles calculation, we propose an interface structure for single triple-layer FeSe on the SrTiO₃(001) surface, a high- T_c superconductor found recently. The key component of this structure is the oxygen deficiency on the top layer of the SrTiO₃ substrate, as a result of Se etching used in preparing the high- T_c samples. The O vacancies strongly bind the FeSe triple layer to the substrate giving rise to a (2×1) reconstruction, as observed by scanning tunneling microscopy. The enhanced binding correlates to the significant increase of T_c observed in experiment. The O vacancies also serve as the source of electron doping, which modifies the Fermi surface of the first FeSe layer by filling the hole pocket near the center of the surface Brillouin zone, as suggested from angle-resolved photoemission spectroscopy measurement.

DOI: [10.1103/PhysRevB.87.220503](https://doi.org/10.1103/PhysRevB.87.220503)

PACS number(s): 74.78.-w, 68.55.Ln, 73.61.-r, 74.62.Dh

High transition temperature (T_c) superconductors were mainly cuprate-based materials.¹ The recent discovery of iron-based superconductors^{2–9} has significantly enriched the family of high- T_c superconductors. Probably of greater importance is that the new iron-based superconductors could serve as a critical test bed for the theories that have been proposed to understand the mechanism of high- T_c superconductivity. Currently, pnictides hold the highest T_c achieved in iron-based superconductors.^{8,9} T_c above liquid nitrogen temperature (77 K), however, has not been realized yet. A recent report of T_c around 77 K from scanning tunneling microscopy (STM) measurement¹⁰ on an iron chalcogenide—namely, FeSe—is particularly interesting and calls for a thorough understanding.

The findings in Ref. 10 are important from at least two aspects. First, the high T_c was observed on one-unit-cell-thick (1 UC) FeSe deposited on the SrTiO₃(001) surface. So, this system represents the simplest building blocks of most high- T_c superconductors, which are usually layered materials.¹ Understanding the mechanism in such a simple system could provide important insights to the understanding of more complex high- T_c superconductors. Second, bulk FeSe has a T_c of only about 8 K.⁷ The drastic increase in T_c after deposition on the SrTiO₃ substrate indicates a critical role of the strong coupling between the 1 UC FeSe and the substrate. In contrast, the deposited FeSe layers thicker than 1 UC do not exhibit high T_c .¹⁰ It is worthwhile to note that such strong coupling could exist in most layered superconductors and be an important component of the mechanism for high- T_c superconductivity.

A thorough understanding of this system requires knowledge of the atomic structures of the 1 UC FeSe layer and its interface with the SrTiO₃ substrate. STM and angle-resolved photoemission spectroscopy (ARPES) have provided some important information on the atomic and electronic structures of this system. From STM measurement, the surface is (2×1) reconstructed.¹⁰ Figure 1 shows an STM image of 1 UC FeSe on SrTiO₃(001). Two domains with a trenchlike boundary can be seen in this image, where one domain exhibits dimers along the [100] direction and the other along the [010] direction.

From ARPES measurement, the Fermi surface of the 1 UC FeSe on the SrTiO₃ substrate does not exhibit a hole pocket at the center of the surface Brillouin zone, which exists in bulk FeSe however.¹¹ In addition to the features above, it has been noted that Se etching before deposition of the FeSe layer is an important step in preparing the high- T_c samples.¹⁰

In this Rapid Communication, by using first-principles calculation we reveal the role of oxygen deficiency at the SrTiO₃ surface in determining the atomic and electronic structures of the FeSe layer. We propose an interface structure that reproduces the above-mentioned features from STM and ARPES experiments. The key component of this structure is O vacancies on the top layer of the SrTiO₃ substrate, which are in accord with the Se etching used to prepare the high- T_c samples. The O vacancies are ordered along the [100] direction and strongly anchor the FeSe layer to the substrate, giving rise to a (2×1) reconstruction. The O vacancies serve as the electron donors, which fill the hole pocket of the Fermi surface of the FeSe layer near the center of the surface Brillouin zone in agreement with the ARPES measurement.

Our calculations are based on density functional theory with the Perdew-Burke-Ernzerhof exchange-correlation functional,¹² as implemented in the VASP code.¹³ Projector augmented wave potentials¹⁴ are used to represent ion cores. Plane waves with an energy cutoff of 400 eV are used as the basis set. The SrTiO₃ substrate is modeled by a ten-atomic-layer slab, which is separated from its periodic images by 12-Å vacuum regions. The surface Brillouin zone is sampled by k -point meshes that are equivalent to the 4×4 Monkhorst-Pack mesh¹⁵ for a (1×1) cell. Atoms in the lower four layers of the SrTiO₃ substrate are fixed at the bulk geometry, while all other atoms are fully relaxed until the residual forces are less than 0.03 eV/Å.

FeSe is a layered material, where a 1 UC FeSe contains a triple layer of FeSe and the binding between the triple layers is from the van der Waals (vdW) interaction. We first studied the deposition of a triple layer of FeSe on a pristine SrTiO₃(001) surface. The SrTiO₃ surface was terminated by a

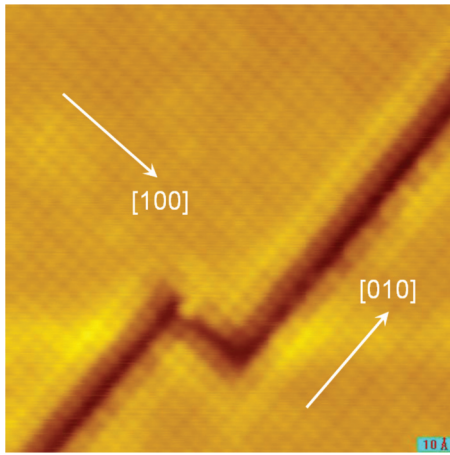


FIG. 1. (Color online) STM image of 1 UC FeSe on the SrTiO₃(001) surface. Two domains are shown, which are separated by a trenchlike structure. One domain exhibits (2 × 1) reconstruction along the [100] direction, while the other one along the [010] direction. The scanning area is 12.8 × 12.8 nm². The bias voltage and tunneling current for obtaining this image are 0.6 V and 46.5 pA, respectively.

TiO₂ layer, as suggested from the experiment.¹⁰ Such a model with (1 × 1) periodicity has been employed in recent studies on this system.^{16–19} Figure 2(a) shows the optimized structure. The thickness of the FeSe layer as measured from the top Ti layer to the top Se layer is 5.65 Å, which is similar to the lattice constant of bulk FeSe ($c = 5.48$ Å) indicating a weak vdW binding. The calculated binding energy is only about 0.05 eV per FeSe unit cell. In order to confirm that we did not miss other possible strong binding configurations, we performed molecular dynamics simulations. The starting structure was very different from the structure in Fig. 2(a),

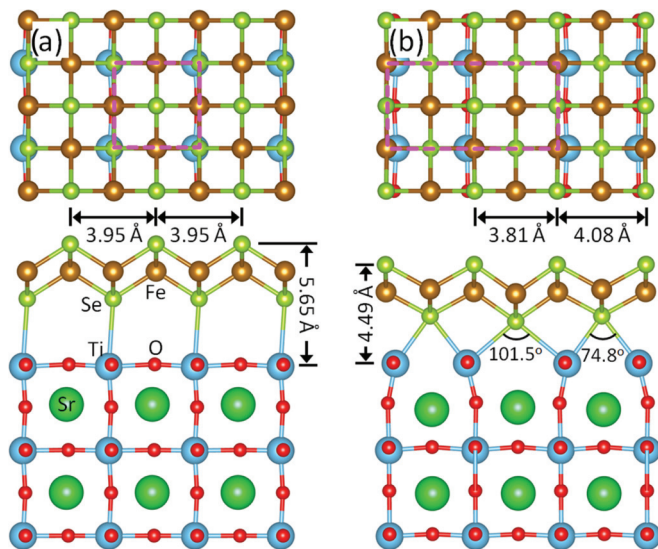


FIG. 2. (Color online) Structural models of 1 UC FeSe (a) on the pristine SrTiO₃(001) surface, which is terminated by a TiO₂ layer and (b) on the O-deficient surface, which is characterized by alternately missing O-atom rows. The top panels show top views, whereas the bottom panels show side views. The surface unit cells are shown in the top views. Several characterizing structural parameters are shown.

but was purposely chosen so that Se-Ti distances are in the typical range of chemical bonds (about 2.6 Å). The simulation was done at 850 K, which is the temperature for deposition of the FeSe layer in experiment.¹⁰ After only 2 ps simulation, we found that the structure already changed back to that in Fig. 2(a).

The results above led us to conclude that the FeSe triple layer does not bind to the pristine SrTiO₃ surface strongly, which is intriguing because the formation of the (2 × 1) reconstruction observed in STM experiments suggests that the first FeSe layer grows epitaxially. The stress built in the epilayer needs to be compensated by a strong binding between the FeSe layer and the substrate. This prompts us to study strong anchoring sites on the SrTiO₃ surface that can bind the FeSe layer more strongly. An important clue from the ARPES measurement is that the FeSe layer is electron doped.^{11,17} Thus, an immediate candidate would be the O vacancies on the SrTiO₃ surface as the O vacancies are usually efficient electron donors in metal oxides, e.g., in TiO₂.²⁰

Given the Se etching used in preparing the high- T_c samples, it is possible that the surface O atoms are replaced by Se atoms. The SrTiO₃(001) surface has two exposed O atoms per unit cell on the top layer. We consider substitution of one or both of the two O atoms by Se. The thermodynamic stability of these substituted surfaces is compared with the pristine surface according to the calculated formation energy per unit cell

$$E_{\text{form}} = E(n\text{Se}_O \text{ on SrTiO}_3) - E(\text{SrTiO}_3) + n\mu_{\text{Se}} - n\mu_{\text{O}},$$

where $E(n\text{Se}_O \text{ on SrTiO}_3)$ and $E(\text{SrTiO}_3)$ are the total energies of the SrTiO₃(001) surface with $n\text{Se}$ substituting for O (denoted as Se_O) and the pristine surface, respectively, and $\mu_{\text{Se}}(\mu_{\text{O}})$ is the chemical potential of Se (O). By definition, the formation energy of the pristine surface is zero. A negative formation energy means that the substituted surface is more stable. Here, we consider a Se-rich condition, i.e., $\mu_{\text{Se}} = E(\text{Se}_2)/2$, where $E(\text{Se}_2)$ is the total energy of a Se₂ molecule. Figure 3(b) shows the formation energy E_{form} as a function of μ_{O} . It can be seen that in the region $-3.6 \text{ eV} < \mu_{\text{O}} < -2.4 \text{ eV}$, the half-substituted surface containing one Se_O per unit cell, as shown in the inset of Fig. 3, becomes more stable than the pristine surface. The surface could even become fully substituted if the growth condition becomes more O poor (i.e., $\mu_{\text{O}} < -3.6 \text{ eV}$). Given the experimental temperature for Se etching of 950 °C and typical ultrahigh vacuum pressure of 10⁻¹² bar, we estimate that μ_{O} is about -3.0 eV ,^{21,22} at which the half-substituted surface is the most stable.

In the subsequent growth of the FeSe layer, the Se-substituted surfaces are the actual substrate. Thus, the Se atoms already existing on the surface can participate in the growth of the first triple layer of FeSe. Because the position of the Se substituting for O coincides with that of the Se in the first triple-layer FeSe, no significant atomic redistribution is necessary. This effectively creates O vacancies at the interface. An interesting finding from our calculations is that after the deposition of a triple-layer FeSe on the half-substituted surface, a (2 × 1) reconstruction becomes more stable, even though in the case without the FeSe layer the unreconstructed (1 × 1) surface is more stable. The optimized structure of the (2 × 1) reconstructed surface is shown in Fig. 2(b), which can be viewed as having alternately missing rows of O atoms

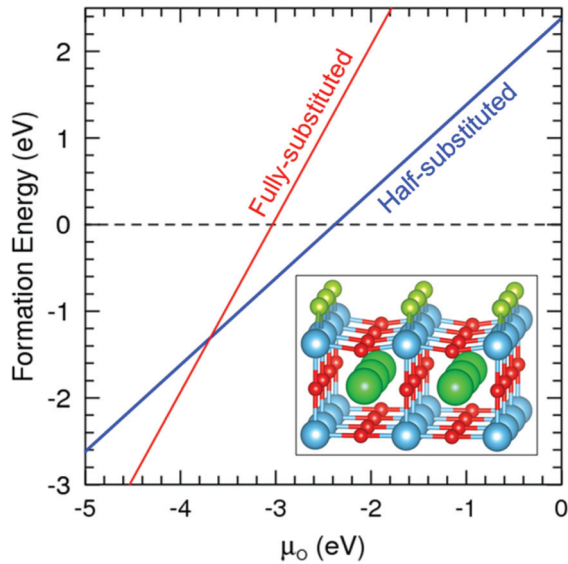


FIG. 3. (Color online) Formation energy of Se substitution of O atoms in the top layer of the TiO_2 -terminated $\text{SrTiO}_3(001)$ surface as a function of O chemical potential, μ_{O} . By definition, the formation energy of the pristine surface without Se substitution is zero, as marked by the dashed line. The inset shows the structure of the half-substituted surface.

(called missing-row structure hereafter). In this structure, there are two different spacings between Se-atom rows on the top layer, which are 4.08 and 3.81 Å, respectively. Another noticeable feature is the significant relaxation in the top layer of Ti atoms, which also form a dimerlike structure. The two Ti-Se-Ti bond angles are 74.8° and 101.5°, respectively, and two Ti-Se bond lengths are 2.97 and 2.71 Å, respectively. Compared with the case of deposition on the pristine surface, the FeSe layer sinks down to the substrate with a thickness of 4.49 Å.

With the interface reconstruction, the binding energy between the FeSe layer and the substrate significantly increases to 0.75 eV per FeSe (1×1) cell according to our calculation. This strong binding is important in determining the growth mode of the FeSe film. To allow stable epitaxial growth of the FeSe layer, the binding energy should be able to compensate the stress built in the epilayer. Otherwise, an incommensurate adlayer will be favored. Our calculation shows that a change in the lattice constant of FeSe by 4.6%, which is the mismatch between the lattice constants of FeSe and SrTiO_3 , results in a total-energy change by 0.28 eV per FeSe (1×1) cell, which is smaller than the binding energy between the FeSe layer and the substrate in our structure. This explains why the first FeSe layer favors epitaxial growth in experiment.

Next, we study the effect of the O vacancy on the Fermi surface of the FeSe triple layer. In Fig. 4(a), we show the band structure for a freestanding FeSe triple layer, where the hole pocket is clearly seen from Γ to about 1/6 of Γ -Y. Bulk FeSe band structure is similar to that in Fig. 4(a). After deposition on the SrTiO_3 surface containing O vacancies, our band-structure calculation shows that the hole pocket is dipped under the Fermi surface of the combined system, as shown in Fig. 4(b), where for clarity we have projected each electronic state in the band structure onto individual atoms and used gray scale

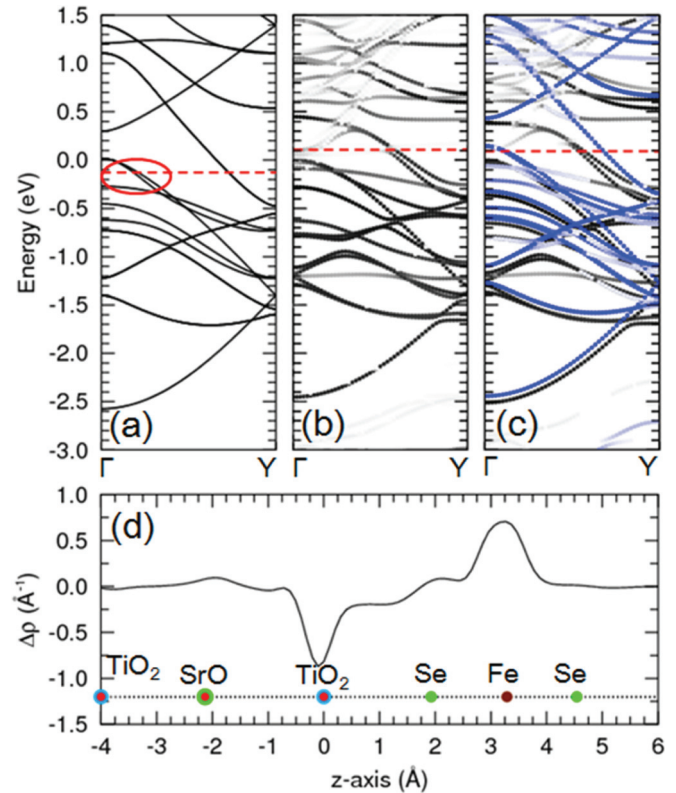


FIG. 4. (Color online) Band structure of (a) a freestanding triple-layer FeSe, (b) one triple layer, and (c) two triple layers of FeSe deposited on the $\text{SrTiO}_3(001)$ surface containing O vacancies. The hole pocket in the freestanding case is marked by a red circle in (a). Each state in (b) and (c) is projected onto the first (in black) or the second (in blue) FeSe layer. The larger the projection, the darker the dot used for that state. Panel (d) shows the charge-density difference obtained by subtracting the valence charge densities of the isolated FeSe layer and SrTiO_3 substrate from that of the combined system. A charge transfer from the top TiO_2 layer to the FeSe layer can be clearly seen.

to represent the contribution from the FeSe layer (the darker, the more contribution from the FeSe layer). Recent ARPES measurement¹¹ shows that the hole pocket at the Γ point, which has been proposed to play a role in the Cooper-pairing mechanism for bulk FeSe within a spin-fluctuation-mediated framework,²³ disappears after being deposited on the SrTiO_3 surface. So, our structure is consistent with the ARPES experiment. The electrons filling the FeSe hole pocket at the Γ point are contributed by the O vacancies. Figure 4(d) shows the charge transfer between the SrTiO_3 substrate and the FeSe layer, as characterized by the charge-density difference ($\Delta\rho$) obtained by subtracting the valence charge densities of the isolated FeSe layer and SrTiO_3 substrate from that of the combined system. From Fig. 4(d), clear charge transfer from the SrTiO_3 substrate to the FeSe layer can be seen, which fills the hole pocket of the FeSe layer and provides strong Coulomb binding between the FeSe layer and the substrate.

Experimentally, the high T_c was only observed on the first FeSe layer, but not on the thicker films.¹⁰ To address this observation, we studied the case with a second layer FeSe deposited on the first layer. In this case, the binding energy

between the first and second layers is found to be 0.03 eV per FeSe (1×1) cell, indicating a pure vdW interaction. This is significantly lower than that between the first layer and the substrate (0.75 eV). Our results thus indicate a clear correlation between the change in T_c and the strength of interface coupling. Interestingly, the hole pocket that is absent on the first layer, reappears at the Γ point on the second layer, as shown in blue in Fig. 4(c).

As a final note, we also considered other known structures of the SrTiO₃(001) surface. Even though a number of reconstructions have been observed on the SrTiO₃(001) surface,^{24–26} we focused on the so-called double-layer-TiO₂ (2×1) surfaces^{27,28} because other more complex surfaces are not compatible with the (2×1) reconstruction under study here. It has been found that, on the double-layer-TiO₂ (2×1) surface, the role of O vacancy is the same as that in the missing-row structure described above.

In summary, the atomic and electronic structures of single triple-layer FeSe deposited on the SrTiO₃(001) surface have

been studied using first-principles calculations. We unveil the critical role of O vacancies at the interface in providing a strong binding and donating electrons to the FeSe layer, which provides important insights to the enhancement of the superconducting transition temperature. An interface structure has been proposed to address the features observed in STM and ARPES experiments. By providing a credible interface structure, our study paves the way for further understanding the mechanism of superconductivity in this important system.

J.B., Y.Y.Z., and S.B.Z. are supported by the US Department of Energy (DOE) under Grant No. DE-SC0002623. Y.Y.S. acknowledges support from the National Science Foundation under Award No. DMR-1104994. The supercomputer time was provided by the National Energy Research Scientific Computing Center under DOE Contract No. DE-AC02-05CH11231 and the Computational Center for Nanotechnology Innovations at Rensselaer Polytechnic Institute.

*suny4@rpi.edu

†qkxue@mail.tsinghua.edu.cn

‡zhangs9@rpi.edu

¹N. Plakida, *High-Temperature Cuprate Superconductors: Experiment, Theory, and Applications* (Springer, Heidelberg, 2010).

²Y. Kamihara, H. Hiramatsu, M. Hirano, R. Kawamura, H. Yanagi, T. Kamiya, and H. Hosono, *J. Am. Chem. Soc.* **128**, 10012 (2006).

³Y. Kamihara, T. Watanabe, M. Hirano, and H. Hosono, *J. Am. Chem. Soc.* **130**, 3296 (2008).

⁴X. H. Chen, T. Wu, G. Wu, R. H. Liu, H. Chen, and D. F. Fang, *Nature (London)* **453**, 761 (2008).

⁵H. Takahashi, K. Igawa, K. Arii, Y. Kamihara, M. Hirano, and H. Hosono, *Nature (London)* **453**, 376 (2008).

⁶M. Rotter, M. Tegel, and D. Johrendt, *Phys. Rev. Lett.* **101**, 107006 (2008).

⁷F.-C. Hsu, J.-Y. Luo, K.-W. Yeh, T.-K. Chen, T.-W. Huang, P. M. Wu, Y.-C. Lee, Y.-L. Huang, Y.-Y. Chu, D.-C. Yan, and M.-K. Wu, *Proc. Natl. Acad. Sci. USA* **105**, 14262 (2008).

⁸Z.-A. Ren, W. Lu, J. Yang, W. Yi, X.-L. Shen, Z.-C. Li, G.-C. Che, X.-L. Dong, L.-L. Sun, F. Zhou, and Z.-X. Zhao, *Chin. Phys. Lett.* **25**, 2215 (2008).

⁹G. Wu, Y. L. Xie, H. Chen, M. Zhong, R. H. Liu, B. C. Shi, Q. J. Li, X. F. Wang, T. Wu, Y. J. Yan, J. J. Ying, and X. H. Chen, *J. Phys.: Condens. Matter* **21**, 142203 (2009).

¹⁰Q.-Y. Wang *et al.*, *Chin. Phys. Lett.* **29**, 037402 (2012).

¹¹D. Liu *et al.*, *Nat. Commun.* **3**, 931 (2012).

¹²J. P. Perdew, K. Burke, and M. Ernzerhof, *Phys. Rev. Lett.* **77**, 3865 (1996).

¹³G. Kresse and J. Furthmüller, *Comput. Mater. Sci.* **6**, 15 (1996).

¹⁴P. E. Blochl, *Phys. Rev. B* **50**, 17953 (1994); G. Kresse and D. Joubert, *ibid.* **59**, 1758 (1999).

¹⁵H. J. Monkhorst and J. D. Pack, *Phys. Rev. B* **13**, 5188 (1976).

¹⁶K. Liu, Z.-Y. Lu, and T. Xiang, *Phys. Rev. B* **85**, 235123 (2012).

¹⁷Y.-Y. Xiang, F. Wang, D. Wang, Q.-H. Wang, and D.-H. Lee, *Phys. Rev. B* **86**, 134508 (2012).

¹⁸F. Zheng, Z. Wang, W. Kang, and P. Zhang, arXiv:1302.2996.

¹⁹T. Bazhiron and M. L. Cohen, *J. Phys.: Condens. Matter* **25**, 105506 (2013).

²⁰A. Janotti, J. B. Varley, P. Rinke, N. Umezawa, G. Kresse, and C. G. Van de Walle, *Phys. Rev. B* **81**, 085212 (2010).

²¹K. Reuter and M. Scheffler, *Phys. Rev. B* **65**, 035406 (2001).

²²Y. Y. Sun, W. Y. Ruan, X. Gao, J. Bang, Y.-H. Kim, K. Lee, D. West, X. Liu, T.-L. Chan, M. Y. Chou, and S. B. Zhang, *Phys. Rev. B* **85**, 195464 (2012).

²³A. Subedi, L. Zhang, D. J. Singh, and M. H. Du, *Phys. Rev. B* **78**, 134514 (2008).

²⁴D. A. Bonnelli and J. Garra, *Rep. Prog. Phys.* **71**, 044501 (2008).

²⁵K. Johnston, M. R. Castell, A. T. Paxton, and M. W. Finnis, *Phys. Rev. B* **70**, 085415 (2004).

²⁶E. Heifets, S. Piskunov, E. A. Kotomin, Y. F. Zhukovskii, and D. E. Ellis, *Phys. Rev. B* **75**, 115417 (2007).

²⁷N. Erdman, K. R. Poepplmeier, M. Asta, O. Warschkow, D. E. Ellis, and L. D. Marks, *Nature (London)* **419**, 55 (2002).

²⁸R. Herger, P. R. Willmott, O. Bunk, C. M. Schlepütz, B. D. Patterson, and B. Delley, *Phys. Rev. Lett.* **98**, 076102 (2007).